Korea-Australia Rheology Journal
Vol. 21, No. 3, September 2009 pp. 161-173

Analysis of conventional drag and lift models for multiphase CFD modeling of blood flow

Fuat Yilmaz and Mehmet Yasar Gundogdu*
University of Gaziantep, Department of Mechanical Engineering, Turkey
(Received July 1, 2009; final version received July 28, 2009)

Abstract

This study analyzes especially drag and lift models recently developed for fluid-solid, fluid-fluid or liquid-liquid two-phase flows to understand their applicability on the computational fluid dynamics, CFD modeling of pulsatile blood flow. Virtual mass effect and the effect of red blood cells, RBCs aggregation on CFD modeling of blood flow are also shortly reviewed to recognize future tendencies in this field. Recent studies on two-phase flows are found as very useful to develop more powerful drag-lift models that reflect the effects of blood cell's shape, deformation, concentration, and aggregation.

Keywords : blood, rheology, CFD, RBC, phase, cell, drag, lift

1. Introduction

Pulsatile blood flow has been of great interest due to interactions observed between vascular diseases and flow patterns through the circulation. Understanding the blood flow mechanics is so important for the development of risk measures on diseases, transport of drugs, and designing more efficient medical devices and equipments. Studies on pulsatile blood flow have been commonly conducted experimentally, theoretically, and computationally. Experimental and theoretical studies on pulsatile pipe flows since the first quarter of the 20th century were reviewed in great detail (Gundogdu and Carpinlioglu, 1999a; Gundogdu and Carpinlioglu, 1999b; Carpinlioglu and Gundogdu, 2001). Medical imaging systems are widely used to display and measure both vessel wall thickness and blood velocities directly in human subjects, but this approach has only been successfully applied to relatively straight vessels due to the limitations such as the implicit assumption of uniform flow (Steinman, 2002; Steinman and Taylor, 2005). In reality, however, most of initiation and progression of vascular diseases occur in complex flow regions. Thus, these regions need more improved techniques for investigation.

Computational methods have widely accepted as a vital means for investigating the blood flow at complex regions. Computational studies, however, include some difficulties such as the mathematical complexity of blood flow dynamics, the requirement on excessive numbers of finite elements to obtain sensitive solutions, and the application of realistic boundary conditions without simplifications, to be solved. Developing an efficient and reliable CFD model for blood flow is thus a hard task. Moreover, CFD models should be validated by accurately chosen and treated experimental data. For nearly three decades, CFD models have, however, been used by investigators to address blood flow because of their advantage in the simplicity of handling a variety of physiological flow conditions by only changing related initial and boundary conditions as well as the possibility of providing information that is hard or even impossible to measure (Stijnen *et al.*, 2004). The CFD models have been found to be an efficient and reliable tool due to the development period during the last few decades. It is likely to continue to play an important role in hemodynamic studies.

The significant and continuous improvements in medical imaging systems, computational techniques, and computer hardware and software performances have also brought to reshape of the CFD modeling for blood flow. The CFD modeling of pulsatile blood flow was initially started with using idealized and averaged artery models together with the Newtonian fluid flow assumption. Later models have, however, included the non-Newtonian fluid rheology together with realistic artery geometries. Recent innovative models; namely, the image-based CFD models including blood flow and its arterial wall, and the multiphase CFD models based on Lagrangian and Eulerian approaches with fluid-solid interaction are now being used. The simultaneous and continuous interaction between the blood flow and the vessel wall constitutes a coupled system and plays a critical role in understanding the mechanisms that lead to various complications in the vascular system. Although these models have provided the means to model this interaction in a more physically realistic manner, its mathematical analysis seems far from complete. Computational simulation in an efficient manner is still one of the major computational challenges. On the other hand, most of the present com-

*Corresponding author: gundogdu@gantep.edu.tr,

putational studies are based on the assumption of blood flow as a single phase. However, on examination, the reality that the blood flow is multiphase becomes readily evident. Blood consists mainly of a dense suspension of elastic red cells in plasma, and its particulate nature is primarily responsible for its unique macroscopic rheology (Yilmaz and Gundogdu, 2008). In the last decade, several multiphase CFD models have been developed to analyze arterial blood flow and clarify the effect of the dispersed particulate phases.

2. Analogy of single- and multi-phase modeling

A great number of single phase CFD models have been proposed to meet the requirements for blood flow in the last few decades. The cell suspended structure of whole blood was ignored and it was simplified as a continuous viscous fluid. For a single phase flow, general conservation equations for mass and momentum can be respectively given as:

$$\frac{\partial \rho}{\partial t} + \nabla \cdot (\rho u) = 0 \tag{1}$$

$$\frac{\partial (\rho u)}{\partial t} + \nabla \cdot (\rho u u) = -\nabla p + \nabla \cdot \tau + \rho g + F \tag{2}$$

where ρ is the density, u is the velocity in axial direction, t is the time, p is the pressure, g is the gravity, F represents external forces, and τ is the extra shear stress tensor defined as:

$$\tau = \mu \frac{du}{dy} \tag{3}$$

where μ is the viscosity of blood. For a Newtonian fluid model, μ is constant and independent of the shear rate. In the case of a non-Newtonian fluid model, μ is a function of shear rate and the shear thinning behavior of blood must also be considered. Viscoelastic models can also be used to describe the elastic behavior of blood as well as its viscous behavior. However, the extra stress tensor includes an elastic stress tensor.

Above a critical shear stress, whole blood has been modeled as a dense mono-dispersion of immiscible and deformable liquid droplets enclosed with an elastic membrane in a Newtonian liquid. However, mono-dispersed structure of red blood cells, RBCs, changes to multi-dispersed structure if the shear rate decreases (Yilmaz and Gundogdu, 2008). Unfortunately, the studies for drag and lift forces acting on mono-dispersed blood cells or rouleaux are very limited in literature. Therefore, the drag and lift models developed for deformable and mobile interface particles such as droplets in a gas-liquid system and bubbles in a liquid-gas system would be very useful for understanding the corresponding behavior of RBCs in blood. The particular loading of RBCs (*i.e.*, the ratio of RBC mass to the plasma mass) is approximately equal to one and represents an intermediate loading case. The phase coupling is so two-way, meaning that there is a mutual effect between the flows of plasma and blood cells. Coupling can take place through mass, momentum, and energy transfer between phases. Otherwise, the particular loading of white blood cells, WBCs, and platelets is less than 1 means that is very low loading case. The coupling between the WBCs or platelets and plasma is so one-way. The plasma carrier influences these types of cells via drag and turbulence, but the WBCs or platelets have no influence on the plasma. However, the continued collisions and hydrodynamic interactions with RBCs results in persistent lateral motion of platelets and WBCs (Kleinstreuer, 2006). There is no mass transfer between plasma and blood cells. Other side, the mass transfer to small diameter branches vessel respect to modeling vessel is generally ignored. Although the blood and the vessel wall continuously exchange substances, the effect of mass transfer from the blood to the vessel tissues is also generally disregarded and mass coupling could be treated as no coupling. Current studies results that blood flow coupled with mass transfer under the effect of hemodynamic parameter are the keys to understand atherosclerosis and as a result the importance of mass transfer at the near wall regions becomes apparent (Chakravarty and Sen, 2005; Soulis *et al.*, 2008). Momentum coupling is the of interaction forces such as drag, lift, virtual mass, and magnus lift forces between the blood cells and plasma phase. The particle response time of blood cells is in the order of 10^{-6} s. Thus, particle Stokes number is less than 1 means that cell and plasma velocity is so close each other. Therefore, RBC velocity approaches the plasma velocity and then particle Reynolds number decrease. As a result of multiphase analysis of blood flow, coupling of RBC with plasma is significant and their effects on each other cannot be ignored. Blood is a single-phase multi-component flow in actual, but for practical purposes it can be treated as a two-phase flow. In recent years, two-phase CFD models have been used to clarify the effects of cell dispersed blood structure on hemodynamic flow conditions. Dispersed flows have been modeled by using either the Lagrangian or the Eulerian approaches in literature. The Lagrangian approach was commonly applied for blood flow to study aggregation and deposition patterns of critical corpuscles such as monocytes and platelets, which play significant roles in arterial disease progression (Buchanan *et al.*, 2000; Hyun *et al.*, 2000a; Hyun *et al.*, 2000b; Hyun *et al.*, 2001; Longest and Kleinstreuer, 2003; Buchanan *et al.*, 2003; Longest *et al.*, 2004; Longest *et al.*, 2005). The effects of the dominant particle phase RBC on cell aggregation and deposition were commonly neglected or limited with a constant dispersion coefficient valid especially in the region of low shear stress. In healthy men, the average

number of red blood cells per cubic millimeter is 5,200,000 (±300,000); in healthy women, it is 4,700,000 (±300,000) (Guyton and Hall, 2006). However, this model is limited to sufficiently low volume fractions and relatively small numbers of blood cells (Jung *et al.*, 2006a). The Lagrangian approach is so impractical to use for such dense suspensions of RBC because of the heavy computational work, and time.

In recent years, Jung *et al.* (Jung *et al.*, 2006a; Jung *et al.*, 2006b; Jung and Hassanein, 2008) and Srivastava and Srivastava (2009) used two-fluid model and an Eulerian-Eulerian model to better analyze the dense suspensions of blood flow. The main difference between two-fluid and the single-phase models is the appearance of the volume fraction for each phase in the conservation equations as well as with coupling among phases by using the mechanisms for the exchange of momentum, heat, and mass. In order to solve the conservation equations for hemodynamics, appropriate rheological properties of each phase must be specified. Eulerian-Eulerian multiphase model can be classified as mixture or heterogeneous mixture models. Heterogeneous mixture models like Eulerian and granular models are especially used for modeling the blood flow. An extension of the SIMPLE algorithm (the phase coupled SIMPLE (PC-SIMPLE) algorithm) is used for the pressure-velocity coupling through these models. Because of the volume occupied by one phase cannot be occupied by other phases, the concept of phasic volume fraction is introduced. In addition, the volume fraction is assumed to be a continuous function of space and time and their sum must be equal to one:

$$\varepsilon_{plasma}+\varepsilon_{RBC}+\varepsilon_{WBC}+\varepsilon_{platelets}=1 \tag{4}$$

In the multiphase, non-Newtonian hemodynamic models, the continuous phase is plasma which contains water, proteins, organic and inorganic substances. The predominant dispersed (particulate) phase in the plasma is RBC at hematocrits of 37~54% in human. Leukocytes or white blood cells (WBC) and platelets occupy a total volume fraction less than one percent in blood and therefore exercise a much smaller effect than RBC on blood rheology. As a result, whole blood flow can be considered as a two-phase flow and shown schematically in Fig. 1. However, multiphase modeling has been used to understand the distribution and effects of the other cells. A general mass balance by the convective mass fluxes without inter-phase mass transfer and mass source for each phase such as plasma, RBC, WBC and platelets is given by:

$$\frac{\partial(\rho_i\varepsilon_i)}{\partial t}+\nabla\cdot(\rho_i\varepsilon_i u_i)=0 \tag{5}$$

where i represents any one of the phases, ρ is the density, ε is the volumetric fraction, t is the time, and u is the velocity. The momentum balance equation for each phase is given by:

$$\frac{\partial(\rho_i\varepsilon_i u_i)}{\partial t}+\nabla\cdot(\rho_i\varepsilon_i u_i u_i)= \tag{6}$$

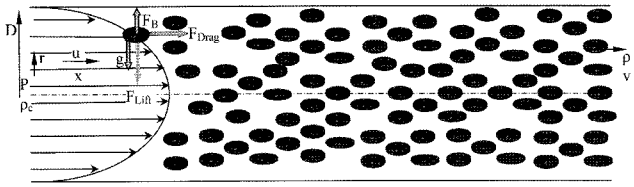

Fig. 1. A schematic representation of two-phase blood flow.

$$-\varepsilon_i\nabla p+\nabla\cdot\tau_i+\varepsilon_i\rho_i g+\sum_{r=1}^{n}R_{ri}+F_i$$

where p is the pressure shared by all phases, τ_i is the i-phase stress-strain tensor, g is the gravity force, and F represents the external forces such as virtual mass, rotational and shear lift, electrical and magnetic forces. R_{ri} is an interaction force between the phase-i and the other phase or phases. In the Newtonian form, the stress-strain tensor for the plasma phase is given as follows:

$$\tau=\varepsilon_p\mu_p(\nabla u_p+(\nabla u_p)^T)+\varepsilon_p\left(\kappa_p-\frac{2}{3}\mu_p\right)\nabla\cdot u_p I \tag{7}$$

where, μ_p and κ_p are the shear and bulk viscosities for the plasma phase, respectively. ε_p is the volume fraction of plasma, and I is a unit tensor. The bulk viscosity, κ_p can be ignored for incompressible fluids. The stress tensor for the particulate phases due to the interactions among particles is given by the form:

$$\tau=-p_i\delta+\varepsilon_i\mu_i(\nabla u_i+(\nabla u_i)^T)+\varepsilon_i\left(\kappa_i-\frac{2}{3}\mu_i\right)\nabla\cdot u_i I \tag{8}$$

where δ is the Kronecker delta and the particle-phase pressure, p_i, represents an inter-particle pressure as a function of volume fraction of the i-phase. This pressure is generated by the kinetic energy of the particle velocity fluctuations and hence collision of cells with each other or elastic or inelastic contact between cells. Since normal blood remains fluid even at a hematocrit of 98% (Fung, 1993) and since WBC and platelets are present at such low volume fraction, the inter-particle pressure of blood can be ignored (Jung and Hassanein, 2008; Jung *et al.*, 2006b). The inter-phase force, R_{ri} depends on the friction, pressure, cohesion, and other effects, and is subject to the conditions that $R_{ri}=-R_{ir}$, and $R_{ii}=0$:

$$\sum_{r=1}^{n}R_{ri}=\sum_{r=1}^{n}K_{ri}(u_r-u_i) \tag{9}$$

where K_{ri} ($=K_{ir}$) is the inter-phase momentum exchange coefficient between the phases. A particle moving in a fluid experiences a drag force due to the viscous effects in the direction of the flow. The RBC has been considered to behave like a liquid droplet without change in the physical characteristics (volume and surface area of RBC) of the membrane (Fischer *et al.*, 1978; Schmid-Schönbein and Wells, 1969). The inter-phase momentum exchange coefficient for liquid-liquid dispersed flow can be written in the following general form:

$$K_{ri} = \frac{\varepsilon_i \varepsilon_r \rho_r f}{\tau_r} \quad (10)$$

where τ_r is the particle relaxation time given as:

$$\tau_r = \frac{\rho_r d_r^2}{18\mu_i} \quad (11)$$

where d_r is the mean diameter of the drops of phase r. The drag function f includes a drag coefficient C_D that is based on the Reynolds number, Re:

$$f = \frac{C_D Re}{24} \quad (12)$$

The drag function, f is always multiplied by the volume fraction of the continuous phase, ε_i as reflected in Eq. (10) to prevent K_{ri}'s tendency to zero whenever the continuous phase is not present within the domain.

3. Drag models

The application of statistically averaged fluid-fluid models for the simulation of blood flow requires the development of adequate models for the inter-phase momentum exchange. This situation comes with a problem at a high phase fraction of the dispersed phase. An accurate modeling of the drag force is a very critical delivery regarding the prediction of mean and turbulent features of two-phase flows, and this problem has provided an appreciable amount of literature. Various models were developed to describe the drag coefficient for fluid-fluid systems as follows:

3.1. Schiller and Naumann Model:

The well-known drag law of Stokes (*i.e.*, C_D=24/Re) proposed for Re<1 was extended for higher particle Re numbers by means of a dimensionless multiplication factor which accounts the inertial effect on the drag force acting on a single non-deformable spherical particle in an infinite stagnant fluid at intermediate Reynolds numbers (Schiller and Nauman, 1935).

$$C_D = \begin{cases} 24(1+0.15Re^{0.687})/Re & Re \le 1000 \\ 0.44 & Re > 1000 \end{cases} \quad (13)$$

where the particle Reynolds number, Re is based on the dispersed particle diameter, d, the magnitude of relative velocity, U_r between the phases, the density, ρ_c and the dynamic viscosity, μ_c of the continuous phase as that:

$$Re = \frac{\rho_c d U_r}{\mu_c} \quad (14)$$

where $U_r = |u - v|$ and u is the velocity of continuous phase and v is the velocity of dispersed phase. The correlation of Schiller and Naumann was also experimentally validated by Klaseboer *et al.* (2001) for a broader variety of liquid-liquid systems with particle Reynolds number as high as 1000. Myint *et al.* (2006) showed that the combination of Schiller and Naumann model and Levich (1962) model including the effects of surfactants and viscosity ratio is appropriate for spheroid drops rising through infinite stagnant liquid at intermediate Reynolds numbers.

3.2. Morsi and Alexander Model:

Morsi and Alexander (1972) also described the drag coefficient for smooth spherical particles as in the Schiller and Naumann model, but with eight different correlations over eight successive ranges of Re. In this model, Re domain is divided into eight successive Re ranges by means of adjusting eight corresponding fits to minimize the deviation between the experimental data and the fitted correlations as that:

$$C_D = a_1 + \frac{a_2}{Re} + \frac{a_3}{Re^2} \quad (15)$$

where Re is defined in Eq. (14). The values of a_1, a_2, and a_3 were evaluated as:

$$a_1, a_2, a_3 \begin{cases} 0, 24, 0 & 0 < Re < 0.1 \\ 3.690, 22.73, 0.0903 & 0.1 < Re < 1 \\ 1.222, 29.1667, -3.8889 & 1 < Re < 10 \\ 0.6167, 46.50, -116.67 & 10 < Re < 100 \\ 0.3644, 98.33, -2778 & 100 < Re < 1000 \\ 0.357, 148.62, -47500 & 1000 < Re < 5000 \\ 0.46, -490.546, 578700 & 5000 < Re < 10000 \\ 0.5191, -1662.5, 5416700 & Re \ge 10000 \end{cases} \quad (16)$$

The particle Reynolds number for realistic suspensions of blood cells was detected to be smaller than unity (*i.e.*, Re<1) (Hyun *et al.*, 2001; Longest *et al.*, 2004, 2005; De Gruttola *et al.*, 2005), so the well-known Stokes formula for the drag coefficient of a spherical solid particle, or more suitable one of the above models at low Reynolds number can be used for RBC in a shear flow. However, the experimental results on drag coefficient of dispersed particles in a liquid-liquid system indicated that the effect of adjacent entities plays a significant role in accurate prediction of drag coefficient at higher concentrations proposed as $\varepsilon > 0.05$ (Al-Taweel *et al.*, 2006) or $\varepsilon \ge 0.1$ (Rusche and Issa, 2000). These types of empirical models take into account the dispersed phase fraction, ε as follows.

3.3. Barnea and Mizrahi Model:

Barnea and Mizrahi (1975) extended a drag coefficient law obtained with solid-fluid systems to liquid-liquid systems using the concept of effective viscosity and a mixture viscosity law similar to a Taylor linear law validated at a high phase fraction. Their model was found as in agreement with 12 different experimental data sources for a wide range of particle Reynolds number and phase fraction.

$$C_D = \left(1+\varepsilon^{\frac{1}{3}}\right)\left(0.63 + \frac{4.8}{\sqrt{Re_m}}\right)^2 \quad (17)$$

where the particle Reynolds number, Re_m is based on the mixture viscosity, μ_m instead of the continuous phase viscosity, μ_c as that:

$$Re_m = \frac{\rho_c d U_r}{\mu_m} \tag{18}$$

where the mixture viscosity, μ_m is evaluated from the following viscosity law:

$$\mu_m = \mu_c K_b \frac{\frac{2}{3}K_b + \frac{\mu_d}{\mu_c}}{K_b + \frac{\mu_d}{\mu_c}} \tag{19}$$

where μ_d is the viscosity of the dispersed phase, K_b and K_a are the empirical functions as follows:

$$K_b = \exp\left(\frac{5\varepsilon K_a}{3(1-\varepsilon)}\right) \tag{20}$$

$$K_a = \frac{\mu_c + 2.5\mu_d}{2.5\mu_c + 2.5\mu_d} \tag{21}$$

3.4. Ishii and Zuber Model:

Ishii and Zuber (1979) derived a drag law by using the same concept of mixture viscosity for particulate flows and gas-liquid systems as well as for liquid-liquid systems, including the case of distorted inclusions.

$$C_D = \frac{24}{Re_m}(1 + 0.1 Re_m^{0.75}) \tag{22}$$

where the particle Reynolds number, Re_m is also based on the mixture viscosity, μ_m as in Eq. (18), but here the mixture viscosity is evaluated from the another mixture viscosity law:

$$\mu_m = \mu_c\left(1 - \frac{\varepsilon}{\varepsilon_{max}}\right)^A \tag{23}$$

where ε_{max} is accepted as 0.62 for solid and 1 for fluid and the exponent A is defined as:

$$A = -2.5\varepsilon_{max}\frac{\mu_d + 0.4\mu_c}{\mu_d + \mu_c} \tag{24}$$

3.5. Kumar and Hartland Model:

Kumar and Hartland (1985) also proposed an empirical drag law for liquid-liquid systems based on a large number of experimental data covering important ranges of particle Reynolds number and phase fraction.

$$C_D = \left(K_1 + \frac{24}{Re}\right)(1 + k\varepsilon^n) \tag{25}$$

where Re is defined as in Eq. (14), $K_1 = 0.53$, $k = 4.56$, and $n = 0.73$.

It is important to note that the above reviewed drag models

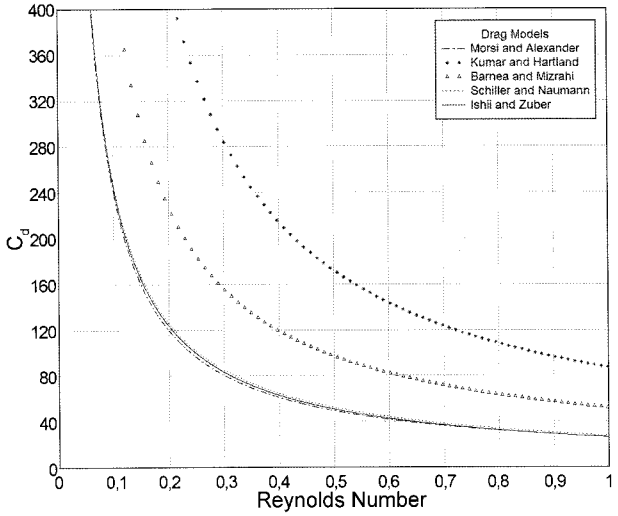

Fig. 2. Comparison of drag models for a fluid-fluid system with $Re < 1.0$ (ε_{RBC}=0.45).

and similar can be used as a local model of the stationary drag term to be introduced into two-phase CFD models. However, the significant discrepancies observed between the proposed drag models raises the question of the choice of a particular drag law for a given liquid-liquid application such as blood flow (Rusche and Issa, 2000). The discrepancies between the all above drag models are shown in Fig. 2 for Reynolds numbers smaller than unity as in the case of blood flow (Hyun *et al.*, 2001; Longest *et al.*, 2004, 2005; De Gruttola *et al.*, 2005). The value of hematocrit, ε_{RBC} is accepted as 0.45 through predictions. It is seen from the figure that; all of the models predict an increase in the drag coefficient when Re decreases. The models of Schiller-Naumann (Eq.13), Morsi-Alexander (Eq.15), and Ishii-Zuber (Eq.22) seem to predict the drag coefficient closely with each other. However, the models of Barnea-Mizrahi (Eq. 17) and Kumar-Hartland (Eq. 25) predict higher drag coefficients than those for same Re numbers. In order to evaluate proper drag law for a liquid-liquid application, it so seems necessary to test it on the basis of statistically averaged local measurements of the drag force. Augier *et al.* (2003) measured the local relative velocity in a homogeneous liquid-liquid flow as a function of the local phase fraction and showed that the above mentioned classical drag coefficient laws underestimate the effect of the phase fraction on the drag coefficient. In return, the actual drag coefficient for a liquid-liquid system can be evaluated as the product of the single drop drag coefficient and a function of the local phase fraction which is well predicted by the theoretical mixture viscosity models in the creeping flow regime. It is so necessary to correlate the drag coefficient for a single sphere as the drag coefficient on systems of spheres at high volume fractions. The drag correlations should so depend on experimental data for a flow with deformable interfaces at high volume fractions (Ishii and Hibiki, 2006). Unfortunately, no data for drag correlation of blood cells are

available in the literature, but a general correlation for liquid-liquid systems would be useful. The Schiller and Nauman model for a single dispersed drop was extended to describe the effect of neighboring entities by using the drag coefficient correlations as that:

$$C_D = C_{D0}F(\varepsilon) \tag{26}$$

where C_{D0} is the drag coefficient of a single spherical drop evaluated from the Schiller and Nauman model (volume fraction of dispersed phase tending towards zero) for a non-uniform flow, and $F(\varepsilon)$ is a function which takes into account the effects arising from the presence of other dispersed elements. The proposed $F(\varepsilon)$ correlation of Rusche and Issa (2000) is that:

$$F(\varepsilon) = e^{K_1\varepsilon} + \varepsilon^{K_2} \tag{27}$$

where the values of the coefficients K_1 and K_2 for spherical droplets were determined respectively as 2.1 and 0.249 by using a non-linear fitting procedure. Another drag function correlation of Augier *et al.* (2003) is also that:

$$F(\varepsilon) = e^{5.2\varepsilon} \tag{28}$$

for $0<\varepsilon<0.4$, and $Re<100$. $F(\varepsilon)$ is here modeled for liquid-liquid systems as a function of the phase volume fraction only. However, further development of these works need to focus on effects of Archimedes, Eötvös or particle Reynolds numbers (Rusche and Issa, 2000; Augier *et al.*, 2003; Behzadi *et al.*, 2004). However in the case of solid-fluid systems, the more specific drag correlations including the effects of both phase fraction and Reynolds number were early achieved and proposed by Wen and Yu (1966) and Wallis (1974) respectively as follows:

$$C_D = \frac{24}{Re}(1+0.15Re^{0.687})(1-\varepsilon)^{-1.7};\quad Re=\frac{(1-\varepsilon)\rho_c dU_r}{\mu_c} \tag{29}$$

$$C_D = C_{D0}(1-\varepsilon)^{3-2n};n = 4.7\frac{1+0.15Re^{0.687}}{1+0.253Re^{0.687}};Re = \frac{\rho_c dU_r}{\mu_c} \tag{30}$$

4. Lift force on dispersed phase

The lift force is a hydrodynamic force acting on a particle dispersed in a shear flow due to the particle rotation. The rotation of particle may be caused by a velocity gradient or may be imposed from some other source such as particle contact and rebound from a surface. The major parameters affecting the lift force acting on a spherical particle in a simple unbounded shear flow are (i) relative velocity between a particle and an ambient fluid, (ii) shear rate of an ambient fluid, (iii) particle rotational speed, and (iv) surface boundary condition (non-slip or slip at particle surface). Multiphase flows always involve some relative motion of one phase with respect to the others; for example, a two-phase flow problem should therefore be formulated in terms of two velocity fields. A general transient two-phase-flow problem can be formulated by using a two-fluid model; however, the greatest difficulty is associated with the establishment of constitutive relations. Additionally, the deformation of a particle causes the associated wake modification and the modified interaction with surrounding flow structures resulting in lift force modification. Thus, the modeling of the lift force in a single deformable particle system is a scientific problem (Ishii and Hibiki, 2006; Hibiki and Ishii, 2007). The lift force acting on dispersed particle is found as significant at higher shear rates and low concentrations (Al-Taweel *et al.*, 2006). The importance of lift force is also pointed for the flows dispersed with larger size particles and especially for quickly separable flow cases (Fluent Inc., 2006). Existing models however assume that the diameter of dispersed particle is much smaller than the inter-particle spacing and thus, the inclusion of lift forces has not yet considered properly for closely packed particles or for very small particles. The lift force acting on a particle due to velocity gradients in the flow field of the continuous phase is normal to the relative direction of flow. Therefore, a cell depleted plasma layer occurs at the wall. Lift forces in high shear rate regions like near wall environment are likely to be important. The particles in high shear rate regions have more mobility than low shear rate regions and as a result experience a reduced drag effect. This effect leads to a modification of the drag coefficient. All of these can influence the particles trajectories and the interaction between particles and the vessel wall.

The research strategy to develop the lift force model and correlation is mainly carried by means of analytical, numerical, and experimental approaches in literature. The analytical calculation of the lift force is very tedious even in asymptotic situations because it requires the consideration of the three dimensional momentum equations without major simplifications. Actually two series of analytical work have been carried out on this problem. The first one considers the effect of an inviscid rotational flow on a sphere and was initiated by Lighthill (1956) and Hall (1956). His results were improved in several subsequent works of Cousins (1970), Auton (1984, 1987), and Naciri (1992). The second series of work concerns low Reynolds number flows and is related to sedimentation problems. Combining several analytical techniques, Saffman (1965, 1968) obtained the lift force on a small rigid sphere in a linear shear flow in the limit of small Reynolds number and large shear.

4.1. Saffman Model:

The Saffman lift force is due to the pressure distribution developed on a particle due to rotation induced by a velocity gradient. His solution is based on a matched asymptotic expansion in which the flow in the inner region is modified by the inertial effects induced by the shear in the outer region. The most common correlation of Saffman's lift model can be given as:

$$F_L = 1.615\rho_c\nu_c^{1/2}d^2(u-v)\left|\frac{du}{dy}\right|^{1/2}\mathrm{sign}\left(\frac{du}{dy}\right) \quad (31)$$

where ρ_c and ν_c are the density and kinematic viscosity of continuous phase, d is the diameter of a spherical particle, u and v are the velocities of the continuous and the dispersed phases in x-direction respectively, and du/dy is the shear rate of the uniform flow field. The correlation requires the conditions that the particle Reynolds number, Re is much less than the shear Reynolds number, Re_G and both Reynolds numbers are much less than unity as given below:

$$Re = \frac{|u-v|d}{\nu_c} = \frac{\rho_c U_r d}{\mu_c} \ll 1; Re_G = \frac{|du\cdot dy|d^2}{\nu_c} \ll 1; \quad (32)$$

$$\beta = \frac{Re_G^{1/2}}{Re} \gg 1; Re_\omega = \frac{\omega d^2}{\nu_c} \ll 1$$

where ω is the rotational speed of the dispersed particle. It can be easily understand that the shear rate always takes a maximum value at the pipe wall and it decreases nearer the high-velocity region around the pipe axis. Saffman's lift force model apparently cannot be applied near the wall, although there might exist a region where it can be applied. As the vessel Reynolds number increases, the dimensions of applicable region are reduced near the axis while the infringement of the constraint becomes severe near the wall. The Saffman's lift force model was therefore modified and extended to overcome its constraints by the several analytical works of McLaughlin (1991, 1993), Mei (1992), Drew and Lahey (1979, 1987, 1990), and Legendre and Magnaudet (1997) as follows.

4.2. McLaughlin Model:

McLaughlin (1991, 1993) extended Saffman's analysis by considering the case where inertia effects related to the mean flow are of same order as those induced by the shear. The restriction on shear magnitude in Saffman's model was relaxed by means of the following expressions for the shear induced lift force on a rigid particle in an unbounded linear shear flow in the low Reynolds number regime:

$$F_L = 1.615\rho_c\nu_c^{1/2}d^2(1-(0.287/\beta^2))(u-v)\left|\frac{du}{dy}\right|^{1/2}\mathrm{sign}\left(\frac{du}{dy}\right); \quad (33)$$

for $\beta \gg 1$

$$F_L = 226.191\rho_c\nu_c^{1/2}d^2\beta^5 ln(\beta^2)(u-v)\left|\frac{du}{dy}\right|^{1/2} sign\left(\frac{du}{dy}\right); \quad (34)$$

for $\beta \ll 1$

for $0.1 \le \beta \le 20$ where β is defined as in Eq.(32). McLaughlin's expressions also require that both Re and Re_G must be small compared to unity (*i.e.*, Re<<1 and Re_G<<1). Legendre and Magnaudet (1997) later reconsidered Saffman's and McLaughlin's analyses for a spherical drop with a vanishing viscosity and found that the lift force is $(2/3)^{1/2}$ times that of a solid sphere.

4.3. Mei Model:

Mei (1992) proposed the following two correlations for a greater range of particle Reynolds number ($0.1 \le Re \le 100$):

$$F_L = 1.615\rho_c\nu_c^{1/2}d^2\{(1-03314\Omega^{1/2})\exp(-Re/10) \quad (35)$$

$$+0.3314\Omega^{1/2}\}(u-v)\left|\frac{du}{dy}\right|^{1/2}\mathrm{sign}\left(\frac{du}{dy}\right)$$

for $Re \le 40$ and;

$$F_L = 1.615\rho_c\nu_c^{1/2}d^2\{0.0524(\Omega Re)^{1/2}\}(u-v)\left|\frac{du}{dy}\right|^{1/2} \quad (36)$$

$$\mathrm{sign}\left(\frac{du}{dy}\right); \mathrm{for} Re \ge 40$$

where finite shear rate, Ω is defined as;

$$\Omega = (Re\beta^2)/2 = Re_G/2Re = (d/2)|du/dy|/|u-v| \quad (37)$$

and it is limited to $0.005 \le \Omega \le 0.4$. He showed that the above empirical equation provided a reasonable fit for Mclaughlin's model. All of the above lift correlations have been derived and proposed assuming an infinite flow field in one direction and with a constant velocity gradient. This assumption can be locally satisfied when the particle is considerably smaller than the dimensions of the vessels such as blood arteries. In micro-vessels, however, the particle diameter is often comparable in size to the vessel diameter. When the velocity gradient can be varied within the scale of particle, the applicability of the correlations is not always assured. Moreover, in the curved regions of the vessel, there appear Dean vortices as secondary flow pattern. The validity of the correlations has not been investigated in such a complicated flow field (Oakawara *et al.*, 2007).

4.4. Drew and Lahey model:

The first attempt in analytically solving the disturbed rotational flow around the sphere was probably carried out by Drew and Lahey (1979) who invoked the frame indifference principle in order to derive a general expression for the force density acting on a dilute suspension of spheres and concluded that the conventional lift coefficient, C_L must equal to the added or virtual mass coefficient, C_{VM} defined by Darwin (1953). Even if the methodologies used by the several groups of authors (Auton, 1987; Drew and Lahey, 1987, 1990, 1993; Zhang and Prosperetti, 1994) are different, their results also converge in suggesting that the identity C_L=C_{VM} holds in inviscid flow (*i.e.*, in the limit of weak shear rates). Moreover, this identity was also found to hold for ellipsoids by Naciri (1992). The proposed lift force model of Drew and Lahey is that:

$$F_L = 0.5236C_L\rho_c d^3(u-v)x(\nabla xu) \quad (38)$$

where C_L is accepted to be constant as 0.5 and equal to C_{VM} for an inviscid flow of an incompressible fluid. Experimental investigations however showed that the lift coefficient values are variable and significantly less than the inviscid value of 0.5, and even negative in some cases (Al-Taweel *et al.*, 2006).

In comparison to the excessive number of above reviewed analytical approaches, the number of numerical studies directed on the lift force acting on a rigid spherical particle dispersed in a shear flow is very limited. Dandy and Dwyer (1990) obtained the first numerical estimates of the lift force for the ranges of the particle Reynolds numbers; $0.01 \leq Re \leq 100$ and the dimensionless shear rate; $0.005 \leq Sr \leq 0.4$ where the particle Reynolds number, Re is defined as in Eq. (14), and the dimensionless shear rate is defined as;

$$Sr = \frac{d}{|u-v|}\left(\frac{du}{dx}\right) \tag{39}$$

The lift coefficient was found approximately constant at a fixed shear rate for Re in the range of $40 \leq Re \leq 100$. Their numerical predictions of the lift force were in good agreement with Saffman's solution but disagreed significantly with McLaughlin's result. While the results of Dandy and Dwyer (1990) show that when the Reynolds number increases the lift coefficient tends towards a constant positive value, those of Kurose and Komori (1996, 1999) display completely different trends: the latter authors find that beyond a certain Reynolds number the lift coefficient becomes negative and depends strongly on the shear rate. Extension of the shear induced lift force on a rigid spherical particle to finite Reynolds numbers, of the order of few hundreds, is through numerical simulations (Bagchi and Balachandar, 2002a, 2002b; Zeng *et al.*, 2009). This situation shows that the situation concerning the lift force on a rigid sphere is not clear at the present time, except in the low Reynolds number limit for which asymptotic results are available. Legendre and Magnaudet (1998) also numerically studied the 3-D flow around a spherical bubble moving steadily in a viscous linear shear flow by solving the full Navier–Stokes equations.

4.5. Legendre and Magnaudet Model:

It was assumed that the bubble surface is clean so that the outer flow obeyed a zero shear stress condition and do not induce any rotation of the bubble. The following correlation for the lift force was developed:

$$F_L = -0.5236 C_L \rho_c d^3 (u-v) x \omega_v \tag{40}$$

for $0.1 \leq Re \leq 500$ and $0.01 \leq Sr \leq 0.25$. Here, ω_v is the vorticity of undisturbed ambient flow at the center of the sphere and the lift coefficient, C_L for a spherical bubble is given by:

$$C_L = \sqrt{\{C_L^{LowRe}(Re, Sr)\}^2 + \{C_L^{HighRe}(Re)\}^2} \tag{41}$$

where the lift coefficients for low and high Re ranges are respectively defined as:

$$C_L^{LowRe}(Re, Sr) = \frac{6}{\pi^2 (2ReSr)^{1/2}} \frac{2.255}{(1+0.1Re/Sr)^{3/2}} \tag{42}$$

$$C_L^{HighRe}(Re) = \frac{1}{2}\left(\frac{1+16Re^{-1}}{1+29Re^{-1}}\right) \tag{43}$$

For a solid particle, the above correlation for C_L at low Re was found approximately valid if it's numerical factor 6 replaced by 27/2. At low Re, the C_L was found strongly dependent on both Sr and Re, and for moderate to high Re such dependence was found to be very weak. Tomiyama (2004) experimentally showed that Legendre and Magnaudet's model was correct for a spherical bubble at Re<5 and at Re<1. However a slight bubble deformation with the aspect ratio in the order of 0.9 caused a noticeable deviation of the measured lift coefficients from the model and further deformation reversed the direction of the lift force acting on a bubble. Takagi and Matsumoto (1995) also pointed out this phenomenon by numerical calculation.

The previous numerical works showed that the lift force was an indispensable factor to reasonably predict the concentration effects that correspond to the experimental results. However, the adopted lift force model of Drew and Lahey (1993) based on Euler–Euler approach, was modified by Ookawara *et al.* (2004, 2005, 2006) in terms of the acting direction and magnitude. By using a similarity hypothesis between the drag and the lift forces, the lift force model of Legendre and Magnaudet (1998) for a single particle system was recently modified to consider the effect of bubble deformation by Hibiki and Ishii (2007) as that:

$$C_L = F(D_d) C_{L0} \tag{44}$$

$$F(D_d) = 2 - \exp(2.92 D_d^{2.21}) \tag{45}$$

where C_{L0} is the lift coefficient for a spherical bubble evaluated from Legendre and Magnaudet's model, $F(D_d)$ is the proposed shape factor for the lift coefficient evaluated by using the experimental data taken by Tomiyama *et al.* (2002), and the dimensionless bubble diameter, D_d was proposed respectively for viscous regime, distorted-particle regime, and spherical-cup bubble regime as follows:

$$D_d = \frac{3^{1/3}}{2^{4/3}} N_\mu^{2/3} Re^{1/3} (1+0.1Re^{3/4})^{1/3}; \tag{46}$$

$$for N_\mu \leq \frac{24\sqrt{2}(1+0.1Re^{0.75})}{Re^2}$$

$$D_d = \frac{1}{4\sqrt{2}} N_\mu Re; for N_\mu \leq \frac{4\sqrt{2}}{Re} \tag{47}$$

$$D_d = \frac{1}{2^{5/3}} N_\mu^{2/3} Re^{2/3}; for N_\mu > \frac{4\sqrt{2}}{Re} \tag{48}$$

where Re is the particle Reynolds number defined as in Eq. (14) with a range; $3.68 \leq Re \leq 78.8$, and N_μ is the viscous number with a range of $0.0435 \leq N_\mu \leq 0.203$, measures the viscous force induced by an internal flow to the surface tension force and defined as that:

$$N_\mu = \frac{\mu_c}{\left(\rho_c \sigma \sqrt{\frac{\sigma}{g\Delta\rho}}\right)^{1/2}} \tag{49}$$

where g is the gravitational acceleration, $\Delta\rho$ is the density difference between the continuous and the dispersed phases, and σ is the surface tension of the bubble. The above modified lift force model in a single particle system was then also extended by Hibiki and Ishii (2007) to a multi-particle system by means of using the particle Reynolds number, Re_m, defined in Eq. (18), based on the mixture viscosity, μ_m, instead the continuous phase viscosity, μ_c. For this purpose, the mixture viscosity was evaluated from the correlation of Ishii and Chawla (1979). The applicability of both the modified and the extended lift force models were qualitatively shown for higher Reynolds numbers, but the validity of the modified lift model on slightly deformable bubbles was limited to $Re \leq 3.68$.

In the experimental approach, experimental data are utilized to obtain an empirical correlation. Starting from the first experiments of Segre and Silberberg (1962a, 1962b), considerable attention has gone to the understanding and quantification of shear induced lift on a particle in relative motion in an unbounded shear flow. Extensive experiments showed that relatively small and large bubbles tend to migrate toward a channel wall and center (Kariyasaki, 1987; Zun, 1988; Liu, 1993; Hibiki and Ishii, 1999; Hibiki *et al.*, 2001, 2003; De Vries *et al.*, 2002; Sankaranarayanan and Sundaresan, 2002; Tomiyama *et al.*, 2002; Tomiyama, 2004; Shew *et al.*, 2006; Kulkarni, 2008). Two most important contributions on the subject among all, come from Tomiyama *et al.* (2002), and Sankaranarayanan and Sundaresan (2002). Tomiyama *et al.* (2002) measured bubble trajectories of single air bubbles in simple shear flows of glycerol–water solutions to evaluate transverse lift force acting on single bubbles. Based on the experimental result, they assumed the lift force caused by the slanted wake had the same functional form as that of the shear induced lift force, and proposed an empirical correlation of the lift coefficient. Very recent experiment done by Tomiyama (2004) implies that a slight bubble deformation might change the direction of the lift force acting on a bubble and of lateral migration even at $Re<5$. The coupling between shear and bubble deformation (whichin turn induces the vorticity/stretching/tilting) induces lateral migration of bubbles and its direction is opposite to that of the spherical bubble. These results agree with the numerical findings by Kariyasaki (1987), Ervin and Tryggvason (1994), and Takagi and Matsumoto (1995), and Bothe *et al.* (2006) for a deforming bubble moving in a shear flow. Thus, in a bubble swarm, even if one ignores the hindrance by surrounding bubbles, for all the bubbles subjected to the same shear and other parameters being constant, the lift coefficient will depend upon the variation in slip velocity and bubble shapes. In majority of the cases, the liquids are never pure and hence the interfacial hydrodynamics gets modified to some extent in terms of the vorticity as well as the pressure variation on the bubble surface. The formulation of C_L for bubbles in a suspension was also derived by Sankaranarayanan and Sundaresan (2002) in terms of dimensionless numbers; namely, the particle Reynolds number, the Eotvos number, the capillary number, and the ratio of slip velocities in two orthogonal directions. The experimental observations of Kulkarni (2008) in a bubble column at different axial levels recently showed that the absolute value of C_L at the center of column is less and it increased toward the wall. Further, except in the vicinity of the wall, $C_L<0$ and it supports the radially inward motion of bubbles.

As described above, the lift and the drag forces are still poorly understood, and thus experimental and numerical efforts have further to be made to get better understanding of them on deformable particles of different sizes, in different flow fields, in dynamic situations, where the particle size would change due to absorption or reaction and also in dispersions. In order to better understanding of the lift and drag forces acting on red blood cells dispersed in plasma of the pulsatile blood flow, the critical studies of Miyazaki *et al.* (1995), Asmolov and McLaughlin (1999), Wakaba and Balachandar (2005), Candelier and Angilella (2006), and Candelier and Souhar (2007) considering the relative velocity between the dispersed particle and the continuous phase takes the form of a time-dependent harmonic function, should be extended for the pulsatile flow case of continuous phase and further combined with the results of above reviewed studies on dispersed deformable bubbles or droplets.

5. Virtual mass effect

The added or virtual mass effect is a concept that occurs when the dispersed phase is subjected to acceleration or deceleration. It is especially significant when the density of dispersed phase is much smaller than the continuous phase density. The virtual mass force can be evaluated from the expression:

$$F_{VM} = C_{VM}\frac{\pi d^3}{6}\rho_c\left(\frac{Du}{dt}-\frac{Dv}{dt}\right);\text{or} \tag{50}$$

$$F_{VM} = C_{VM}\frac{\pi d^3}{6}\rho_c\left\{\left(\frac{\partial u}{\partial t}+(u\cdot\nabla)u\right)-\left(\frac{\partial v}{\partial t}+(v\cdot\nabla)v\right)\right\}$$

where C_{VM} is the virtual mass coefficient and the term D/dt denotes the material time derivative. The well-known equality between the virtual mass coefficient and the lift

coefficient holds only in the limit of weak shears and nearly steady flows (Drew and Lahey, 1979, 1987, 1990; Zhang and Prosperetti, 1994; Cockljat, 2000). The value of C_{VM} is generally accepted as 0.5 for inviscid flows. Experimental investigations however showed that its value is variable and significantly less than the inviscid value of 0.5, and even negative in some cases (Al-Taweel *et al.*, 2006). Jung *et al.* (2006b) and Srivastava and Srivastava (2009) proposed in their numerical analyses that the estimated shear induced lift and virtual mass forces for blood flow are negligible.

6. Aggregation of blood cells

The bridging due to the adsorption of macromolecules onto adjacent cell surfaces, and the depletion due to the osmotic gradient arising from the exclusion of macromolecules near the cell surface, are presently used as molecular models to describe the aggregation behaviors of RBC (Baumler *et al.*, 1999; Meiselman *et al.*, 2007). Moreover, the predicted effects of blood composition, cellular properties and clinical conditions on aggregation (Rampling *et al.*, 2004; Meiselman *et al.*, 2007), the measured aggregation tendencies (Shin *et al.*, 2009), and the predictions on interaction forces between RBCs (Tha and Goldsmith, 1986, 1988; Tees *et al.*, 1993; Zhu, 2000) have been used to understand the aggregation behavior. The effects of RBC aggregation on hemodynamics and on the other blood cells have also been investigated (Goldsmith *et al.*, 1999; Baskurt and Meiselman, 2007). Note that the most of the previously reviewed drag and lift models suppose that the dispersed phase particle is spherical, rigid, and having an immobile interface. RBC in blood plasma is however a biconcave disc-shaped deformable particle and it can be deformed isochorically without any change in surface area or volume. One of the important factors affecting the shape of RBC is shear rate. At lower shear rates, RBC suspension is a multi-dispersed system which contains so many aggregate parts (rouleaux) of various sizes. The shear dependent mechanisms of RBC aggregation are figured out by the balance of aggregation and disaggregation forces. However, this mechanisms and exact role of aggregation on blood flow remain unclear. Disaggregation forces mainly consist of mechanical shear force, repulsive force, and elastic force potential of RBC membrane. Above a critical shear stress, the system becomes mono-dispersed, consisting of single cells, as RBC aggregates have broken up. Schmid-Schönbein and Wells (1969) observed the fluid drop-like behavior of single RBC. While under shear, the cells become progressively deformed into prolate ellipsoids, their long axis aligned parallel to the direction of flow, the elongation increasing with increasing shear stress. The rotational motion of its membrane about cell interior, called as tank treading motion, is also observed. The shape of RBC, whether prolate ellipsoid, biconcave disc or rouleaux, thus depends upon the shear stress and affects the drag and lift forces acting. Therefore, a dynamic shape factor is necessary to account this effect on an individual and aggregated RBCs. Jung and Hassanein (2008) recently proposed the following dynamic shape factor, F_s for the realistic range of shear rate in plasma at which RBC aggregates exist:

$$F_s = 1.5\left(1+\left(\lambda\frac{du}{dy}\right)^2\right)^{0.058697} \tag{51}$$

where λ is the time constant with the value as 0.11sec. This dynamic shape factor is limited to the shear rates smaller than 300 sec^{-1}. Above this limit, no expressions for a dynamic shape factor in blood can be found in the literature. A shape factor can be further derived experimentally from microscopic images of the RBC by using a high speed camera for flow at higher shear rates. Using available images, one can also evaluate shape factors for RBC of regular shape (*i.e.*, prolate ellipsoid or ellipsoid). A shear rate dependent correlation can then be formed from these shape factors. It is expected that the degree of deformability of the RBC and the plasma viscosity will have dominant effects on the shape factor.

7. Conclusions

This paper is presented as an insight into the CFD modeling of two-phase blood flow. It can be concluded that the role of CFD modeling in blood flow studies is very critical and expected to continue in future. Recently, several multiphase CFD models based on Lagrangian and Eulerian approaches have been used as a means of characterizing realistic blood flow. The Lagrangian approach is applicable to blood flow modeling at relatively small concentrations of cells. The Eulerian approach, however, seems to be more suitable than the Lagrangian approach for dense suspensions of blood cells. Some critical conclusions to be useful for two-phase CFD modeling of blood flow are also derived from the upcoming investigations on conventional multiphase flows:

1. Drag and lift forces acting on blood cells are important for a realistic modeling of blood flow. Both drag and lift force models used in the present limited number of multiphase CFD models however neglect the presence of neighboring entities and suppose that the RBC is a spherical and rigid particle, and its membrane is immobile. The present review on fluid-solid and fluid-fluid or especially liquid-liquid two-phase flows has however indicated that the recently developed drag force models include the effects of dispersed particle shape and concentration, and the lift force models also include the effects of particle shape. As an initial attempt, these models can be adopted on multiphase modeling of blood flow. Moreover, the

deformation, concentration, and aggregation behaviors of actual RBC at different shear rates and plasma viscosities should be further experimentally investigated so as to form more realistic drag and lift models over physiological ranges of effective parameters. The effect of tank treading motion (*i.e.*, mobility of RBC membrane) on the drag and lift forces especially at high shear rates should also be clarified.

2. The present review on two-phase flows also shows that lift force acting on dispersed particles causes to the lateral migration of particles in a flow vessel, so it plays a key role on the traveling trajectory of dispersed particle and in the homogeneity of dispersed phase in vessel. The present multiphase CFD models of blood flow, however, do not consider the lift force or consider with a limited effect by means of using a fixed lift coefficient with the value of 0.5, accepted as equal also to the virtual mass coefficient.

Acknowledgements

This study is supported by the Research Fund of the University of Gaziantep in terms of a research project coded as MF.07.06.

References

Al-Taweel, A.M., S. Madhavan, K. Podila, M. Koksal, A. Troshko and Y.P. Gupta, 2006, CFD Simulation of Multiphase Flow: Closure Recommendations for Fluid-Fluid Systems, *12th European Conference on Mixing*, Bologna, Italy, June 27-30.

Augier, F., O. Masbernat and P. Guiraud, 2003, Slip velocity and drag law in a liquid-liquid homogeneous dispersed flow, *AIChE J.* **49**, 2300-2441.

Auton, T.R., 1987, The lift force on a spherical body in a rotational flow, *J. Fluid Mech.* **183**, 199-218.

Auton, T.R., 1984, The dynamics of bubbles, drops and particles in motion in liquids, PhD Dissertation, University of Cambridge.

Asmolov, E.S. and J.B. McLaughlin, 1999, The inertial lift on an oscillating sphere in a linear shear flow, *Int. J. Multiphase Flow* **25**, 739-751.

Bagchi, P. and S. Balachandar, 2002a, Effects of free rotation on the motion of a solid sphere in linear shear flow at moderate Re, *Phys. Fluids* **14**, 2719-2737.

Bagchi, P., and S. Balachandar, 2002b, Shear versus vortex-induced lift force on a rigid sphere at moderate Re, *J. Fluid Mech.* **473**, 379-388.

Barnea, E. and J. Mizrahi, 1975, A generalized approach to the fluid dynamics of particulate systems. Part 2: sedimentation and fluidization of clouds of spherical liquid drops, *Can. J. Chem. Eng.* **53**, 461-468.

Baskurt, O.K. and H.J. Meiselman, 2007, Hemodynamic effects of red blood cell aggregation, *Indian J. Exp. Biol.* **45**, 25-31.

Baumler, H., B. Neu, E. Donath and H. Kiesewetter, 1999, Basic phenomena of red blood cell rouleaux formation biorheology, *Biorheology* **36**, 439-442.

Behzadi, A., R.I. Issa and H. Rusche, 2004, Modelling of dispersed bubble and droplet flow at high phase fractions, *Chem. Eng. Sci.* **59**, 759-770.

Bothe, D., Schmidtke, M. and Warnecke, H.-J., 2006. VOF-simulation of the lift force for single bubbles in a simple shear flow, *Chem. Eng. and Techn.* **29**, 1048-1053.

Buchanan, J.R., C. Kleinstreuer and J.K. Comer, 2000, Rheological effects on pulsatile hemodynamics in a stenosed tube, *Comput. Fluid.* **29**, 695-724.

Buchanan, J.R., C. Kleinstreuer, S. Hyun and G.A. Truskey, 2003, Hemodynamics simulation and identification of susceptible sites of atherosclerotic lesion formation in a model abdominal aorta, *J. Biomech.* **36**, 1185-1196.

Candelier, F., and J.R. Angilella, 2006, Analytical investigation of the combined effect of fluid inertia and unsteadiness on low-Re particle centrifugation, *Phys. Rev. E* **73**, 047301.

Candelier, F. and M. Souhar, 2007, Time-dependent lift force acting on a particle moving arbitrarily in a pure shear flow at small reynolds numbers, *Phys. Rev. E* **76**, 067301.

Carpinlioglu, M.O. and M.Y. Gundogdu, 2001, A critical review on pulsatile pipe flow studies directing towards future research topics, *Flow. Meas. and Instrum.* **12**, 163-174.

Chakravarty, S. and S. Sen, 2005, Dynamic response of heat and mass transfer in blood flow through stenosed bifurcated arteries, *Korea Aust. Rheol. J.* **17**, 47-62.

Cousins, R.R., 1970, A note on the shear Flow past a sphere, *J. Fluid Mech.* **40**, 543-547.

Dandy, D.S. and Dwyer, H.A., 1990, A sphere in shear flow at finite Reynolds number: effect of shear on particle lift, drag, and heat transfer, *J. Fluid Mech.* **216**, 381-410.

Darwin, C. 1953, Note on hydrodynamics, *Cambiridge Phil. Trans.* **49**, 342-354.

De Gruttola, S., K. Boomsma and D. Poulikakos, 2005, Computational simulation of a non-Newtonian model of the blood separation process, *Artif. Organs* **29**, 949-959.

De Vries, A.W.G., A. Biesheuvel and L. van Wijngaarden, 2002, Notes on the path and wake of a gas bubble rising in pure water, *Intl. J. of Multiphase Flow* **28**, 1823-1835.

Drew, D. and R.T. Lahey, 1979, Applications of general constitutive principles to the derivation of multidimensional two-phase flow equations, *Intl J. Multiphase Flow* **5**, 243-264.

Drew, D. and R.T. Lahey, 1987, The virtual mass and lift force on a sphere in rotating and straining inviscid flow, *Intl J. Multiphase Flow* **13**, 113-121.

Drew, D. and R.T. Lahey, 1990, Some supplemental analysis concerning the virtual mass and lift force on a sphere in a rotating and straining flow, *Intl J. Multiphase Flow* **16**, 1127-1130.

Drew, D. and R.T. Lahey, 1993, Analytical modeling of multiphase flow, *Particulate Two-Phase Flow*, Butterworth-Heinemann, Boston, 509-566.

Ervin, E.A. and G. Tryggvason, 1994, The rise of bubbles in a vertical shear flow, In: Proceedings of the ASME Winter Meeting, Fluids Engineering Div., Chicago.

Fischer, T.M., M. Stöhr-Liesen and H. Schmid-Schönbein, 1978, The red cell as a fluid droplet: tank tread-like motion of the human erythrocyte membrane in shear flow, *Science* **202**, 894-896.

Fluent User's Guide, ver. 6.3.26, Fluent Inc., 2006.
Fung, Y.C., 1993, *Biomechanics: Mechanical Properties of Living Tissues*, Second Edition, Springer-Verlag, New York.
Goldsmith, H.L., D.N. Bell, S. Spain and F.A. McIntosh, 1999, Effect of red blood cells and their aggregates on platelets and white cells in flowing blood, *Biorheology* **36**, 461-468.
Gundogdu, M.Y. and M.O. Carpinlioglu, 1999a, Present state of art on pulsatile flow theory, part 1. laminar and transitional flow regimes, *JSME Int. J.* **42**, 384-397.
Gundogdu, M.Y., and M. O. Carpinlioglu, 1999b, Present state of art on pulsatile flow theory, part 2. turbulent flow regime, *JSME Int. J.* **42**, 398-410.
Guyton, A.C. and J.E. Hall, 2006, *Textbook of Medical Physiology*, Eleventh Edition, Elsevier Saunders.
Hall, I.M., 1956, The displacement effect of a sphere in a two-dimensional flow. *J. Fluid Mech.* **1**, 142-161.
Hibiki, T., and M. Ishii, 1999, Experimental study on interfacial area transport in bubbly two-phase flows, *Intl J. of Heat and Mass Transfer* **42**, 3019-3035.
Hibiki, T., M. Ishii and Z. Xiao, 2001, Axial interfacial area transport of vertical bubbly flows, *Intl J. of Heat and Mass Transfer* **44**, 1869-1888.
Hibiki, T., R. Situ, Y. Mi and M. Ishii, 2003, Local flow measurements of vertical upward bubbly flow in an annulus, *Intl J. of Heat and Mass Transfer* **46**, 1479-1496.
Hibiki, T., and M. Ishii, 2007, Lift force in bubbly flow systems, *Chem. Eng. Sci.* **62**, 6457-6474.
Hyun, S., C. Kleinstreuer and Jr. J.P. Archie, 2000a, Hemodynamics analyses of arterial expansions with implications to thrombosis and restenosis, *Med. Eng. Phys.* **22**, 13-27.
Hyun, S., C. Kleinstreuer and J.P. Archie, 2000b, Computer simulation and geometric design of endarterectomized carotid artery bifurcations, *Crit. Rev. Biomed. Eng.* **28**, 53-59.
Hyun, S., C. Kleinstreuer and Jr. J.P. Archie, 2001, Computational particle hemodynamics analysis and geometric reconstruction after carotid endarterectomy, *Comput. Biol. Med.* **31**, 365-384.
Ishii, M. and T.C. Chawla, 1979, Local drag laws in dispersed two-phase flow, Argonne National Laboratory Report, ANL-79-105 (NUREG/CR-1230).
Ishii, M., and N. Zuber, 1979, Drag coefficient and relative velocity in bubbly, droplet or particulate flows, *AIChE J.* **25**, 843-855.
Ishii, M. and T. Hibiki, 2006, *Thermo-fluid Dynamics of Two-phase Flow*, Springer, New York.
Jung, J. and A. Hassanein, 2008, Three-phase CFD analytical modeling of blood flow, *Med. Eng. Phys.* **30**, 91-103.
Jung, J., R.W. Lyczkowski, C.B. Panchal and A. Hassanein, 2006a, Multiphase hemodynamic simulation with pulsatile flow in a coronary artery, *J. of Biomech.* **39**, 2064-2073.
Jung, J., A. Hassanein and R.W. Lyczkowski, 2006b, Hemodynamic computation using multiphase flowdynamics in a right coronary artery, *Ann. Biomed. Eng.* **34**, 393-407.
Kariyasaki, A., 1987, Behavior of a single gas bubble in a liquid flow with a linear velocity profile. Proceedings of the 1987 ASME/JSME Thermal Engineering Conference, 261-267.
Klaseboer, E., J.P. Chavaillier, A. Mate, O. Masbernat, and C. Gourdon, 2001, Model on experiments of drop impinging on an immersed wall, *Phys. Fluids* **13**, 45-57.
Kleinstreuer, C., 2006, *Biofluid Dynamics: Principles and Selected Applications*, CRC Pres.
Komori, S. and R. Kurose, 1996, The effects of shear and spin on particle lift and drag in shear flow at high Reynolds numbers, *Advances in Turbulence VI,* (ed. S. Gavrilakis, L. Machiels and P. Monkewitz), Kluwer, 551-554.
Kulkarni, A.A., 2008, Lift force on bubbles in a bubble column reactor: Experimental analysis, *Chem. Eng. Sci.* **63**, 1710-1723.
Kumar, A., and S. Hartland, 1985, Gravity settling in liquid-liquid dispersions, *Can. J. Chem. Eng.* **63**, 368-376.
Kurose, R., and S. Komori, 1999, Drag and lift forces on a rotating sphere in a linear shear flow, *J. Fluid Mech.* **384**, 183-206.
Legendre, D. and J. Magnaudet, 1997, A note on the lift force on a spherical bubble or drop in a low-Reynolds-number shear flow, *Physics of Fluids* **9**, 3572-3574.
Legendre, D. and J. Magnaudet, 1998, The lift force on a spherical bubble in a viscous linear shear flow, *J. Fluid Mech.* **368**, 81-126.
Levich, V.G., 1962, *Physicochemical Hydrodynamics*, Prentice-Hall, New York.
Lighthill, M.J., 1956, Drift, *J. Fluid Mech.* **1**, 31-53.
Liu, T.J., 1993, Bubble size and entrance length effects on void development in a vertical channel, *Intl J. of Heat and Mass Transfer* **19**, 99-113.
Longest, P.W. and C. Kleinstreuer, 2003, Comparison of blood particle deposition models for non-parallel flow domains, *J. Biomech.* **36**, 421-430.
Longest, P.W., C. Kleinstreuer and J.R. Buchanan, 2004, Efficient computation of micro-particle dynamics including wall effects, *Comput. Fluid.* **33**, 577-601.
Longest, P.W., C. Kleinstreuer and A. Deanda, 2005, Numerical simulation of wall shear stress and particle-based hemodynamic parameters in pre-cuffed and streamlined end-to-side anastomoses, *Ann. Biomed. Eng.* **33**, 1752-1766.
McLaughlin, J.B., 1991, Inertial migration of a small sphere in linear shear flows, *J. Fluid Mech.* **224**, 261-274.
McLaughlin, J.B., 1993, The lift on a small sphere in wall-bounded linear shear flows, *J. Fluid Mech.* **246**, 249-265.
Mei, R., C.J. Lawrence and R.J. Adrian, 1991, Unsteady drag on a sphere at finite Reynolds number with small-amplitude fluctuations in the free-stream velocity, *J. Fluid Mech.* **233**, 613-631.
Meiselman, H.J., B. Neu, M.W. Rampling and O.K. Baskurt, 2007, RBC aggregation: Laboratory data and models, *Indian J. Exp. Biol.* **45**, 9-17.
Miyazaki, K., D. Bedeaux and J. Bonet Avalos, 1995, Drag on a Sphere in a Slow Shear Flow, *J. Fluid Mech.* **296**, 373-390.
Morsi, S. A. and A. J. Alexander, 1972, An investigation of particle trajectories in two-phase flow systems, *J. Fluid Mech.* **55**, 193-208.
Myint, W., S. Hosokawa and A. Tomiyama, 2006, Terminal velocity of single drops in stagnant liquids, *Journal of Fluid Science and Technology* **1**, 72-81.
Naciri, M.A., 1992, Contribution à l'étude des forces exercées par un liquide sur une bulle de gaz: portance, masse ajoutée et interactions hydrodynamiques, Ph.D. Thesis, L'ecole Centrale de Lyon, France.

Ookawara, S., D. Street and K. Ogawa, 2004, Practical application to micro-separator/classifier of the Euler-granular model, In: International Conference on Multiphase Flow 2004, Yokohama, Japan.

Ookawara, S., D. Street and K. Ogawa, 2005, Quantitative prediction of separation efficiency of a micro-separator/classifier by Euler-granular model, In: A.I.Ch.E. 2005 Spring National Meeting, Atlanta.

Ookawara, S., D. Street and K. Ogawa, 2006, Numerical study on development of particle concentration profiles in a curved microchannel, *Chemical Engineering Science* **61**, 3714-3724.

Oakwara, S., M. Agrawal, D. Street and K. Ogawa, 2007, Quasi-direct numerical simulation of lift force-induced particle separation in a curved microchannel by use of a macroscopic particle model, *Chemical Engineering Science* **62**, 2454-2465.

Rampling, M.W., H.J. Meiselman, B. Neu and O.K. Baskurt, 2004, Influence of cell-specific factors on red blood cell aggregation, *Biorheology* **41**, 91-112.

Rusche, H. and R.I. Issa, 2000, The effect of voidage on the drag force on particles in dispersed two-phase flow, *Japanese European Two-Phase Flow Meeting*, Tsukuba, Japan.

Saffman, P.G., 1965, The lift force on a small sphere in a slow shear flow, *J. Fluid Mech.* **22**, 385-400.

Saffman, P.G., 1968, Corrigendum to "The lift on a small sphere in a slow shear flow", *J. Fluid Mech.* **31**, 624.

Segre, G. and A. Silberberg, 1962a, Behaviour of macroscopic rigid spheres in Poiseuille flow. Part 1. Determination of local concentration by statistical analysis of particle passages through crossed light beams, *J. Fluid Mech.* **14**, 115-135.

Segre, G. and A. Silberberg, 1962b, Behaviour of macroscopic rigid spheres in Poiseuille flow. Part 2. Experimental results and interpretation, *J. Fluid Mech.* **14**, 136-157.

Schiller, L. and Z. Naumann, 1935, A Drag Coefficient Correlation, *Z. Ver. Deutsch. Ing.* **77**, 318-320.

Schmid-Schönbein, H. and R. Wells, 1969, Fluid drop-like transition of erythrocytes under shear, *Science* **165**, 288-291.

Shew, W.L., S. Poncet and J.F. Pinton, 2006, Force measurements on rising bubbles, *J. Fluid Mech.* **569**, 51-60.

Shin, S., Y. Yang and J.S. Suh, 2009, Measurement of erythrocyte aggregation in a microchip stirring system by light transmission, *Clini.l Hemorheo. and Microcirc.* **41**, 197-207.

Soulis, J.V., G.D. Giannoglou, V. Papaioannou, G.E. Parcharidis and G.E. Louridas, 2008, Low-density lipoprotein concentration in the normal left coronary artery tree, *Biomedical Engineering On Line* **7**, 26.

Srivastava, V.P. and R. Srivastava, 2009, Particulate suspension blood flow through a narrow catheterized artery, *Computers and Mathematics with Applications* **58**, 227-238.

Steinman, D.A., 2002, Image-based computational fluid dynamics modeling in realistic arterial geometries, *Ann. Biomed. Eng.* **30**, 483-497.

Steinman, D.A. and C.A. Taylor, 2005, Flow imaging and computing: Large artery hemodynamics, *Ann. Biomed. Eng.* **33**, 1704-1709.

Stijnen, J.M.A., J. de Hart, P.H.M. Bovendeerd and F.N. van de Vosse, 2004, Evaluation of a fictitious domain method for predicting dynamic response of mechanical heart valves, *J. Fluid. Struct.* **19**, 835-850.

Sankaranarayanan, K. and S. Sundaresan, 2002, Lift force in bubbly suspensions, *Chemical Engineering Science* **57**, 3521-3542.

Takagi, S. and Y.Matsumoto, 1995, Three dimensional calculation of a rising bubble. In: Proceedings of the Second International Conference on Multiphase Flow, Kyoto.

Tees, D.F.J., O. Coenen and H.L. Goldsmith, 1993, Interaction forces between red-cells agglutinated by antibody. 4. Time and force dependence of break-up, *Biophys. J.* **65**, 1318-1334.

Tha, S.P. and H.L. Goldsmith, 1986, Interaction forces between red-cells agglutinated by antibody. 1. Theoretical, *Biophys. J.* **50**, 1109-1116.

Tha, S.P. and H.L. Goldsmith, 1988, Interaction forces between red-cells agglutinated by antibody. 3. Micromanipulation, *Biophys. J.* **53**, 677-687.

Tomiyama, A., H. Tamai, I. Zun and S. Hosokawa, 2002, Transverse migration of single bubbles in simple shear flows, *Chemical Engineering Science* **57**, 1849-1858.

Tomiyama, A., 2004, Drag, lift and virtual mass forces acting on a single bubble, Proceedings of the Third International Symposium on Two-phase Flow Modeling and Experimentation, Pisa, Italy, 22-24.

Wakaba, L. and S. Balachandar, 2005, History force on a sphere in a weak linear shear flow, *Int. J. Multiphase Flow* **31**, 996-1014.

Wallis, G.B., 1974, The terminal speed of single drops or bubbles in an infinite medium, *Int. J. Multiphase Flow* **1**, 491-511.

Wen, C. and Y. Yu, 1966, Mechanics of Fluidization, *Chem. Eng. Prog. Symp. Ser.* **62**, 100-110.

Yilmaz, F. and M.Y. Gundogdu, 2008, A critical review on blood flow in large arteries; relevance to blood rheology, viscosity models, and physiologic conditions, *Korea Aust. Rheol. J.* **20**, 197-211.

Zeng, L., F. Najjar, S. Blachandar and P. Fischer, 2009, Force on a finite-sized particle located close to a wall in a linear shear flow, *Phys. Fluids* **21**, 033302.

Zhu, C., 2000, Kinetics and mechanics of cell adhesion, *J. of Biomech.* **33**, 23-33.

Zhang, D. Z. and Prosperetti, A., 1994, Averaged equations for inviscid disperse two-phase flow. *J.Fluid Mech.* **267**, 185-219.

Zun, I., 1988, Transition from wall void peaking to core void peaking in turbulent bubbly flow, *Transient Phenomena in Multiphase Flow*, Hemisphere, Washington, 225-245.